MAREK MARCZEWSKI

ORCID: 0000-0002-2728-5363

WŁODZIMIERZ TYLUS

ORCID: 0000-0001-6780-5100

JULIUSZ WINIARSKI*

ORCID: 0000-0003-0761-1579

Group of Surface Technology, Department of Advanced Material Technologies, Faculty of Chemistry, Wrocław University of Science and Technology, Wrocław, Poland

* Corresponding author

DOI: 10.15199/40.2024.4.2

The effect of anodic polarization of 304 stainless steel in choline chloride-based DES solvent on its surface morphology and corrosion resistance

Wpływ polaryzacji anodowej stali nierdzewnej 304 w rozpuszczalniku DES na bazie chlorku choliny na morfologię powierzchni i odporność na korozję

AISI 304 alloy steel was polarized anodically in a deep eutectic solvent based on choline chloride and oxalic acid (1 : 1 molar ratio) at the temperature range of 25–75°C and the current density range of 2.5–45 mA cm^{-2}. No improvement in visual parameters (gloss) was observed with increasing temperature. That was due to the formation of numerous pits on the surface as evidenced by SEM microscopy. AFM showed at lower temperatures the evenly distributed shallow pits, while at higher temperatures – less numerous but larger ones. XPS and ICP-AES analysis showed that the anodic polarization process increased the content of oxidized chromium on the surface and indicated high degree of iron leaching from the material. Morphology of this passive layer, which thickness was calculated to 3.3 nm, was characterized by uniform mixture of Cr(III) oxide and hydroxide. In contrast to chemically etched steel, polarization in DES produced surface layer enriched with Cr_2O_3 (56% instead of 28% total share) with lower share of $Cr(OH)_3$ (41% instead of 70% total share). Anodic polarization process in proposed DES was responsible for a slight increase in corrosion resistance of 304 steel.

Keywords: stainless steel, electropolishing, anodic polarization, deep eutectic solvents (DES), passive layer, XPS, EIS, SEM, AFM

Stal stopową AISI 304 poddano polaryzacji anodowej w rozpuszczalniku eutektycznym złożonym z chlorku choliny i kwasu szczawiowego (1 : 1 molowo) w temperaturze 25–75°C i przy gęstości prądu 2,5–45 mA cm^{-2}. Nie zaobserwowano poprawy połysku wraz ze wzrostem temperatury procesu ze względu na powstanie licznych wżerów na powierzchni, widocznych za pomocą mikroskopii SEM. Analiza AFM wykazała, że w niższych temperaturach wżery są płytkie i równomiernie rozmieszczone, a w wyższych są większe i mniej liczne. Analizy XPS i ICP-AES ujawniły, że na skutek polaryzacji anodowej wzrasta ilość utlenionego chromu w powierzchni stali, czemu towarzyszy nadmierne roztwarzanie żelaza ze stopu. Morfologia wytworzonej warstwy pasywnej, o grubości około 3,3 nm, to jednorodna mieszanina tlenku i wodorotlenku Cr(III). W porównaniu z trawioną chemicznie stalą polaryzacja anodowa w DES skutkuje wytworzeniem warstwy powierzchniowej wzbogaconej w Cr_2O_3 (56% zamiast 28% zawartości) i z mniejszym udziałem $Cr(OH)_3$ (41% zamiast 70%). Proces polaryzacji anodowej stali 304 w zaproponowanym DES przyczynił się do poprawy odporności na korozję.

Słowa kluczowe: stal nierdzewna, polerowanie elektrochemiczne, polaryzacja anodowa, rozpuszczalniki eutektyczne, warstwa pasywna, XPS, EIS, SEM, AFM

Mgr inż. Marek Marczewski, Ph.D. student in Group of Surface Technology, Department of Advanced Material Technologies, Faculty of Chemistry, Wrocław University of Science and Technology. Research area: electroplating and corrosion.
E-mail: marek.marczewski@pwr.edu.pl

Dr hab. inż. Włodzimierz Tylus, prof. PWr., Group of Surface Technology, Department of Advanced Material Technologies, Faculty of Chemistry, Wrocław University of Science and Technology. Research area: surface engineering, catalysis, XPS.
E-mail: wlodzimierz.tylus@pwr.edu.pl

Dr hab. inż. Juliusz Winiarski, prof. PWr., Head of the Group of Surface Technology, Department of Advanced Material Technologies, Faculty of Chemistry, Wrocław University of Science and Technology. Research area: electroplating, coating testing, corrosion issues, electrochemistry, electrode materials, ionic liquids.
E-mail: juliusz.winiarski@pwr.edu.pl

Received / Otrzymano: 4.10.2023. Accepted / Przyjęto: 30.01.2024

1. Introduction

Alloy steel is one of the most willingly used materials in the food industry [1, 2]. This is due to its high resistance to corrosion, which is very important when in contact with potentially corrosive food products, as well as its relative inertness in relation to food [3] and well known processing [4]. In order to further improve the parameters of stainless steel, its surface is often modified, e.g. in the polishing process. By leveling the irregularities present on the steel surface, filth caused by the presence of food products are easier to remove, and they are not able to stick to the surface. This is very important, because food residues can contribute to local corrosion, and thus damage to installations or tools, which can lead to contamination of food with metallic elements. Food scraps collected in this way can also be a breeding ground for bacteria and fungi that can threaten the health of humans and animals. Among all the methods used to reduce roughness, one of the most commonly used methods in the production of food-contact apparatus is electrochemical polishing [5, 6]. In addition to reducing the roughness of steel, the electrochemical polishing process leads to the enrichment of the surface layer with chromium and nickel, which are elements that improve the corrosion resistance of steel. This process is normally carried out in electrolytes composed of a mixture of strong sulfuric and nitric acids [7, 8]. They are very effective and cheap to produce, but their use has a number of disadvantages.

According to the increasingly widespread concept of "green chemistry", one of the elements that can be modified in the discussed process is the use of a less invasive solvent, which would have operating parameters similar to standard baths [9]. One of the potential electrolytes are ionic liquid analogues belonging to the group of deep eutectic solvents (DES) [10]. These solvents are used in electrochemical processes due to their desirable operating parameters, such as: high current efficiency, low aggressiveness, and negligible amount of generated gases on the electrode/liquid interface [11–14]. The bath used in this way would meet the principles of "green chemistry" and would make it possible to remove one of the factors generating pollution. Unfortunately, the current disadvantages of these solvents are high viscosity at temperatures close to the room temperature, which can significantly hinder rinsing processes.

The aim of this study was to investigate whether a DES based on choline chloride and oxalic acid, in a molar ratio of 1 : 1, can be effectively used as a substitute for standard baths in electrochemical polishing of 304 alloy steel. The advantages of this DES include low crystallization temperature, high conductivity (relative to other DES solvents) and very low harmfulness of the liquid compared to standard acid baths [15]. Preliminary studies of the anodic polarization process of steel in this solution promised the effective performance of the process [16], however, i.e., copper electrodeposition [17] or electrochemical polishing of nickel alloys [18] are also possible.

The analysis made it possible to determine changes in the surface properties of 304 steel after electrochemical treatment, such as roughness and corrosion resistance, but also to determine how selective the process is in relation to alloying components. The current parameters needed to carry out the anodic polarization were determined with linear sweep voltammetry (LSV). Changes in surface morphology were studied with scanning electron microscope (SEM). To determine changes in the chemical composition of the steel surface and the composition of the produced passive layers the X-ray photoelectron spectroscopy (XPS) technique was used. The surface topography of steel samples was initially examined using the contact profilometry method, and on the nanoscale using the atomic force microscope (AFM). Corrosion resistance tests were carried out in 0.5 mol dm^{-3} solution of NaCl with the use of direct current polarization techniques, which include electrochemical impedance spectroscopy (EIS) and linear polarization resistance (LPR) technique. The selectivity of the leaching of the alloy components into the eutectic solvent was determined by atomic emission spectrometry (ICP-AES).

2. Experimental section

2.1. Materials and sample preparation

AISI 304 alloy steel substrate with a 2B surface finish (unpolished, cold rolled) was chosen in the shape of 1.5 mm thick discs with diameter of 14.8 mm. This type of steel typically contains: 66.74–71.24% Fe, 17.5–19.5% Cr, 8–10.5% Ni, 2% Mn, 1% Si, 0.11% N, 0.07% C, 0.05% P, and 0.03% S [19]. The samples were degreased in methanol in an ultrasonic bath (reference sample, hereinafter referred to as "as-delivered"), then mechanically grinded with sandpaper #600, and chemically etched (solution consisting of: 10% HNO_3 by volume, 20% HCl and 70% deionized water) for 60 s at 25°C.

The eutectic solvent (DES) was prepared via mixing choline chloride (ChCL; 2-hydroxyethyltrimethylammonium chloride ≥98%, Sigma, as supplied) with oxalic acid (OA; Merck Emplura) in a 1 : 1 molar ratio. This process was carried out at a temperature of 85°C until a uniform, transparent liquid was obtained. The tested liquid conductivity was 4.2 mS cm^{-1} at the temperature of 35°C, which is a value similar to that obtained in the literature [20].

The anodic polarization process was carried out in a glass vessel with a water jacket, filled with 100 cm^3 of eutectic solvent in the temperature range from 25°C to 75°C for 5 min. Rectangular platinized titanium electrodes with dimensions of 30 × 70 mm were used as cathodes. After electrochemical treatment, the tested samples were cleaned in demineralized water, methanol and finally dried. The samples were stored in a vacuum desiccator. The current densities at which the process was carried out were selected on the basis of linear sweep voltammetry measurements.

2.2. Research methods

The Interface 1010E (Gamry) potentiostat was used for linear sweep voltammetry (LSV) measurements, which were carried out directly in the DES bath at 25–75°C. Measurements were conducted in a volume of 50 cm^3 of the solvent with a scan rate of 20 mV s^{-1}, starting from the open circuit potential (E_{OC}) and ending at a voltage of +3 V vs E_{OC}. The reference electrode was made of silver wire (99.9%, Sigma), while the platinum sheet electrodes with dimensions of 8 × 50 mm (99.99% Pt) were used as the cathodes. All potentials presented in this work are referred to Ag quasi-reference electrode. The SEM Quanta 250 (FEI) scanning electron microscope was used for analysis of surface morphology. The photos were taken at a tilt of 50° to the electron gun, with an accelerating voltage of 10 kV. The content of alloying elements in galvanic baths before and after the anodic polarization process was analyzed with the ICP-AES iCAP 7400 atomic emission spectrometer (Thermo Scientific). Corrosion resistance was measured using electrochemical impedance spectroscopy (EIS) and linear polarization resistance (LPR) methods. Measurements were conducted at 22°C during 24 h of exposure to

deaerated 0.5 mol dm^{-3} solution of NaCl in a 400 ml corrosion cell (Metrohm), with measurements taken every hour. Pt counter electrode and a reference electrode Ag|AgCl (3 mol dm^{-3} KCl, Metrohm) installed in a Luggin capillary were used. Every LPR measurement was carried out in the range from −10 mV to +10 mV to the E_{OC}, with a scan rate 1 mV s^{-1}. After 24 h potentiodynamic polarization curves were recorded from −0.1 to +0.8 V, relative to the E_{OC}, with a scan rate set to 0.167 mV s^{-1}. EIS spectra were recorded at E_{OC} from 100 kHz to 1 mHz, with 10 mV alternating current amplitude and 10 pts./dec. Geometric surface of the working electrode was 1 cm^2 for all measurements.

The X-ray photoelectron spectroscopy (XPS) was used for the chemical analysis of the surface. SPECS PHOIBOS 100 spectrometer was used, equipped with a non-monochromatized Al source of emission (1486.7 eV), operating at 250 W for high resolution spectra. Surface etching during XPS measurements was carried out by Ar^+ sputtering with the beam energy of 4 keV and a beam current density of 7.5 µA cm^{-2}. SPECLAB software was used to analyze the spectra using a Gaussian-Lorenzian curve profile and a Shirley baseline. The C 1s peak at 284.8 eV was used as the reference.

Analysis of the topography and surface roughness of the steel was performed with a DektakXT contact profilometer (Bruker), equipped with a 12.5 µm tip, using the Vision64 software (Bruker), and the PN-EN ISO 4287:1999 and PN-EN ISO 11562:1998 standards. Analysis of the sample topography on the nano-scale was performed using the Nanosurf FLEX-Axiom atomic force microscope (AFM) in a contact mode. The obtained data was processed in the Gwyddion program.

3. Results and discussion

3.1. Voltammetric measurements

In order to determine the parameters in which the oxidation takes place on the surface of 304 steel, LSV measurements in the temperature range from 25°C to 75°C were carried out. The temperature range chosen for analysis corresponds to temperatures used in anodic polarization process performed in standard acid baths [21]. According to the obtained results (Fig. 1), the oxidation process of 304 steel surface took place at a potential close to 0 V vs Ag for each of the temperatures. However, with the increase in temperature, the transition point to the passive state moved towards negative values, from 1.0 V to 0.6 V vs Ag. Based on the LSV experiment, it was decided to perform the anodic polarization process with representative potential values for each of the graphs. More precisely, it was decided to determine three values for each of the curves by equating the tangents to the parts of the graphs showing the oxidation process of the steel surface, as demonstrated in Fig. 1 for the curve "75°C". Then, two extreme values of the potential equal to the tangents were determined as the point with the lowest (referred to as polarized at low current densities) and highest (referred to as polarized at high current densities) current parameters for the conducted process, and the value between them (referred to as polarized at "medium current densities"), which were used to determine the desired anodic current density, which lay between 2.5 mA cm^{-2} and 45 mA cm^{-2} (Table 1).

According to Table 1, in the temperature range from 25°C to 55°C, a certain trend can be noticed that the application of the highest current density reduces the overall roughness of the sample, which may be the result of an increase in the kinetics of the surface oxidation process. However, between individual samples, the R_a parameter is not much changed. However, the rapid increase in roughness is noticeable at the two highest temperatures, i.e., 65°C and 75°C. Then the increase in the current density leads to a significant increase in the R_a (even to 339 nm), which may indicate the formation of a large number of pits on the surface.

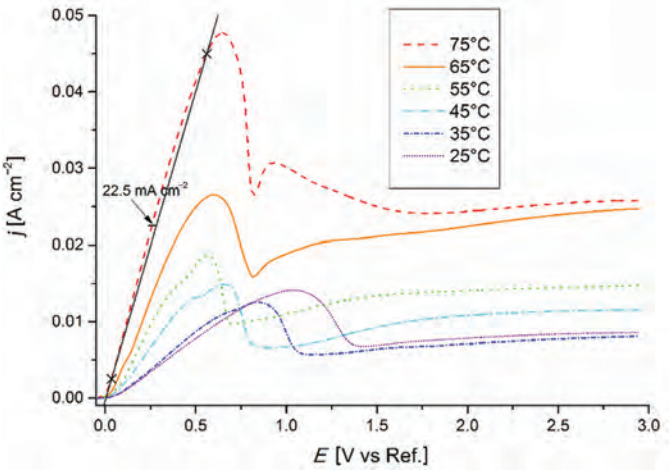

Fig. 1. LSV curves for AISI 304 steel, recorded in the DES of choline chloride and oxalic acid at temperatures from 25°C to 75°C in the potentials range from E_{OC} to 3 V vs Ag at a scan rate of 20 mV s^{-1}

Rys. 1. Woltamogramy LSV zarejestrowane dla stali AISI 304 w mieszaninie DES złożonej z chlorku choliny i kwasu szczawiowego w temperaturach od 25°C do 75°C w zakresie potencjałów od E_{OC} do 3 V wzgl. Ag przy szybkości 20 mV s^{-1}

Table 1. Current parameters selected for samples undergoing anodic polarization based on Fig. 1, and R_a parameter values for tested samples, determined by the contact profilometry method

Tabela 1. Parametry prądowe dobrane dla próbek poddanych polaryzacji anodowej na podstawie rys. 1 oraz wartości parametrów R_a dla badanych próbek, wyznaczone metodą profilometrii stykowej

Temperature, T [°C]	Potential, E [V vs Ag]	Current density, j [mA cm^{-2}]	Roughness, R_a [nm]
25	0.20	2.5	21 ±7
	0.50	8.5	28 ±10
	0.80	12.5	25 ±7
35	0.15	2.5	16 ±3
	0.40	7.5	27 ±10
	0.65	11.0	19 ±8
45	0.15	2.5	22 ±7
	0.30	8.5	25 ±10
	0.50	13.0	19 ±6
55	0.15	2.5	28 ±10
	0.35	11.0	25 ±9
	0.50	17.5	21 ±6
65	0.05	2.5	12 ±4
	0.25	15.0	26 ±7
	0.50	25.0	53 ±15
75	0.05	2.5	15 ±4
	0.30	22.5	33 ±17
	0.55	45.0	339 ±137

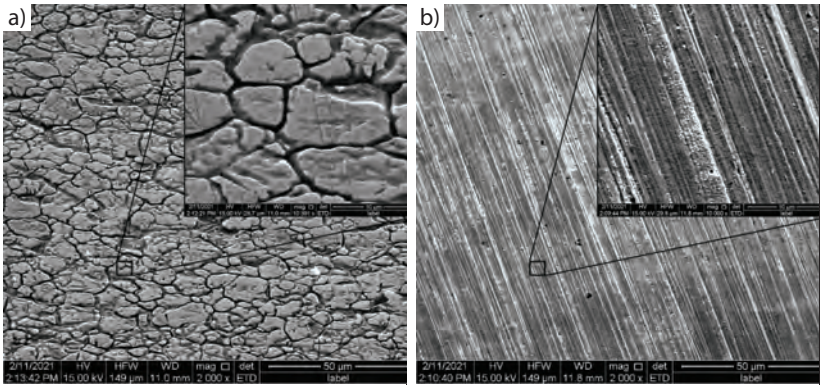

Fig. 2. Surface morphology of 304 steel: a) "as-delivered", b) after mechanical grinding and chemical etching for 60 s at 25°C

Rys. 2. Morfologia powierzchni stali 304: a) w stanie, w jakim została dostarczona, b) po szlifowaniu mechanicznym i trawieniu chemicznym przez 60 s w temperaturze 25°C

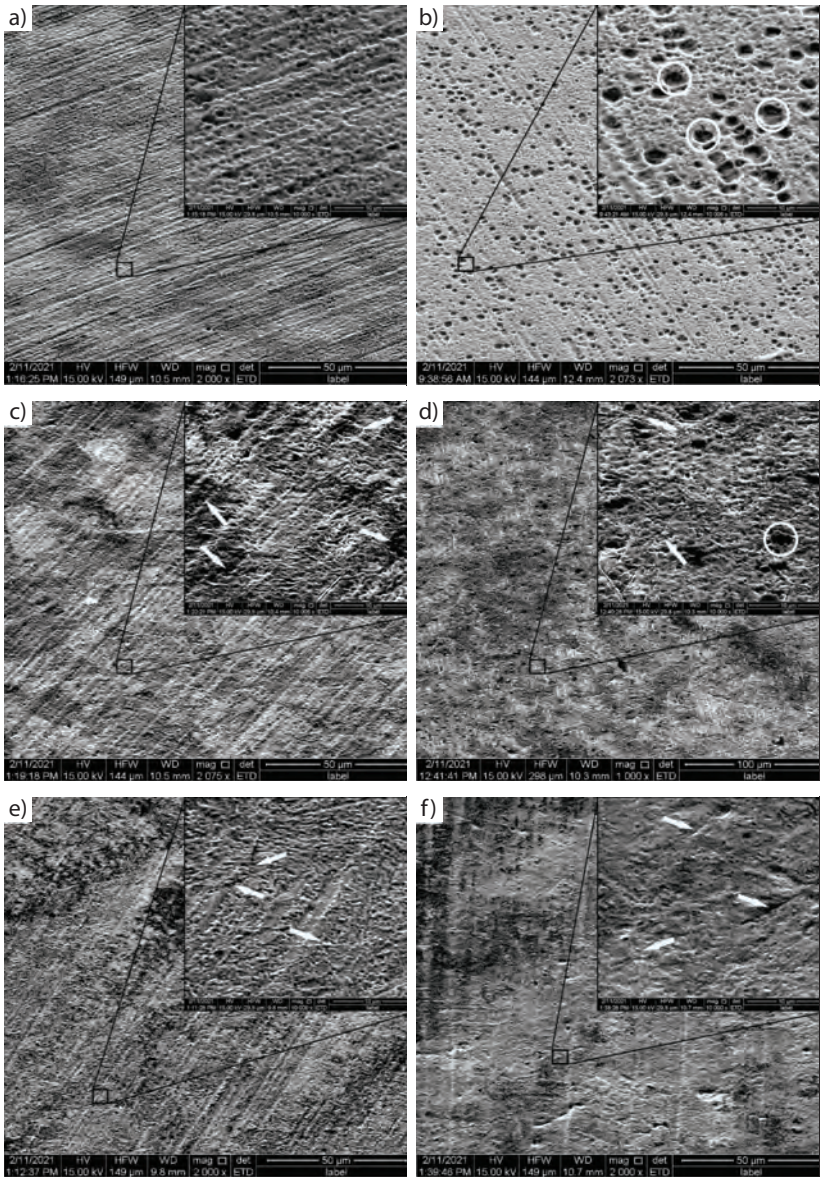

Fig. 3. The surface morphology of AISI 304 steel after anodic polarization process with the following parameters: a) T = 25°C, j = 8.5 mA cm^{-2}, b) T = 35°C, j = 7.5 mA cm^{-2}, c) T = 45°C, j = 8.5 mA cm^{-2}, d) T = 55°C, j = 11.0 mA cm^{-2}, e) T = 65°C, j = 15.0 mA cm^{-2}, f) T = 75°C, j = 25.0 mA cm^{-2}

Rys. 3. Morfologia powierzchni stali AISI 304 po procesie polaryzacji anodowej o następujących parametrach: a) T = 25°C, j = 8,5 mA cm^{-2}, b) T = 35°C, j = 7,5 mA cm^{-2}, c) T = 45°C, j = 8,5 mA cm^{-2}, d) T = 55°C, j = 11,0 mA cm^{-2}, e) T = 65°C, j = 15,0 mA cm^{-2}, f) T = 75°C, j = 25,0 mA cm^{-2}

3.2. Surface morphology and topography

The "as-delivered" 304 steel sample had visible austenite grains with slightly marked rolling lines resulting from the course of the manufacturing process (Fig. 2a). After surface grinding, only grinding lines were observed (Fig. 2b). In the visible photograph, it can be seen that the additional chemical etching caused a slight blurring of the cut line, but this did not significantly affect the morphology. These reference samples became the basis for further analysis of changes occurring on the surface after anodic polarization.

Analysis of the samples polarized at medium current densities (between 7.5 mA cm^{-2} and 22.5 mA cm^{-2}, Table 1), it was possible to observe more and more etchings and pitting on the surface at lower temperatures (Fig. 3a and 3b), which are not a desired phenomenon in the electropolishing process. Again, the gradual disappearance of the grinding lines and the progressive etching of the grain surface and boundaries can be seen as the temperature increases (Fig. 3c–3e). Particularly noticeable grain boundary etching could be observed at the highest process temperatures (Fig. 3f), which is related to the increased kinetics of the reaction compared to polarizations carried out at temperatures close to room temperature. However, when analyzing samples polarized at these medium current densities, while the great variation in surface morphology could be noticed, it was without a sudden increase in the roughness parameter.

The next stage of the analysis of the modification of the surface topography was to determine the change in the parameter R_a, which is the arithmetic mean deviation of the profile from the mean line. In the case of steel "as-delivered", the R_a value was 124 ±8 nm, and it served as the reference value for other samples. The surface of 304 steel samples after grinding and chemical etching had a much lower R_a value (18 ±8 nm, Table 1). The reduction of the roughness was influenced by the removal of the present scratches and surface imperfections in the machining process. Steel samples after the polarization process were characterized by different values of the R_a parameter, which are presented in Table 1. In a few cases (the sample subjected to the anodic polarization process at a temperature of 65°C at a current density of 2.5 mA cm^{-2} showed the lowest roughness, equal to 12 ±4 nm), it was possible to obtain a roughness value lower than that of the sample as delivered, but the microscopic photos showed that even the samples showing a lower R_a parameter had numerous pits. Macroscopically, the samples did not show any greater surface gloss and the ability to reflect light.

Roughness analysis, limited by the stylus profiler capabilities, was complemented by an analysis made with an atomic force microscope (AFM) and only for the samples anodically polarized at

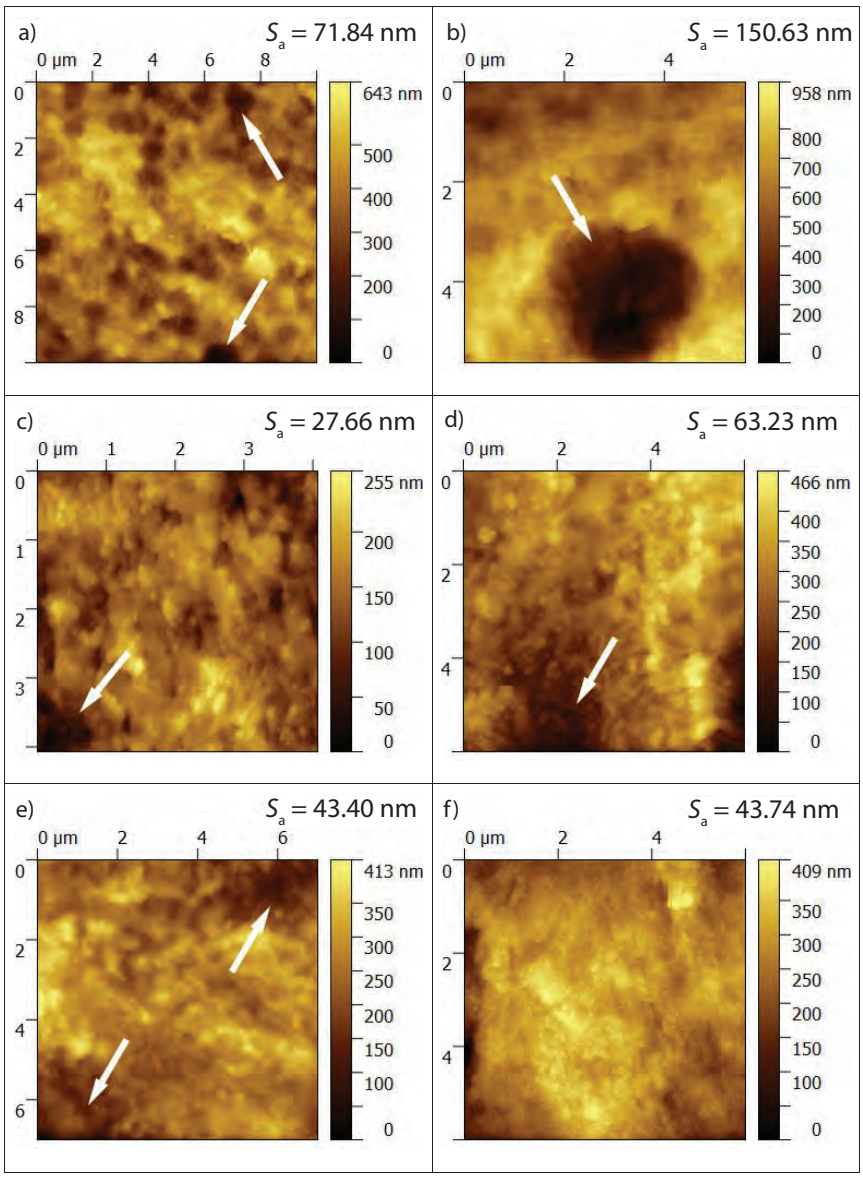

Fig. 4. AISI 304 steel topography after anodic polarization process with the following parameters: a) T = 25°C, j = 8.5 mA cm^{-2}, b) T = 35°C, j = 7.5 mA cm^{-2}, c) T = 45°C, j = 8.5 mA cm^{-2}, d) T = 55°C, j = 11.0 mA cm^{-2}, e) T = 65°C, j = 15.0 mA cm^{-2}, f) T = 75°C, j = 25.0 mA cm^{-2}

Rys. 4. Topografia powierzchni stali AISI 304 po procesie polaryzacji anodowej o następujących parametrach: a) T = 25°C, j = 8,5 mA cm^{-2}, b) T = 35°C, j = 7,5 mA cm^{-2}, c) T = 45°C, j = 8,5 mA cm^{-2}, d) T = 55°C, j = 11,0 mA cm^{-2}, e) T = 65°C, j = 15,0 mA cm^{-2}, f) T = 75°C, j = 25,0 mA cm^{-2}

Table 2. Content of alloying elements in DES solvents before and after 5 min polarization of 304 steel at various temperatures and medium current densities (according to Table 1)

Tabela 2. Zawartość pierwiastków stopowych w rozpuszczalnikach DES przed polaryzacją i po 5-minutowej polaryzacji stali 304 w różnych temperaturach przy średnich gęstościach prądu (zgodnie z danymi przedstawionymi w tabeli 1)

Condition of samples	Elemental content [ppm]						
	Fe	Cr	Ni	Mn	Fe : Cr	Fe : Ni	Cr : Ni
Before anodic polarization	<0.23	<0.01	0.05	0.97	19 : 1	4.5 : 1	1 : 4.3
After polarization at 25°C	6.61	1.15	0.761	1.86	5.7 : 1	8.7 : 1	1.5 : 1
After polarization at 35°C	12.80	2.38	1.33	2.16	5.4 : 1	9.6 : 1	1.8 : 1
After polarization at 45°C	13.40	2.35	1.76	2.10	5.7 : 1	7.6 : 1	1.3 : 1
After polarization at 55°C	33.10	5.15	3.55	1.96	6.4 : 1	9.3 : 1	1.4 : 1
After polarization at 65°C	32.70	5.82	3.25	1.73	5.6 : 1	10.1 : 1	1.8 : 1
After polarization at 75°C	50.70	9.24	4.94	2.38	5.5 : 1	10.3 : 1	1.9 : 1

the medium current densities. AFM measurements allowed to determine the differentiation of the surface topography, presented in Fig. 4, along with the S_a roughness parameters. In the case of the sample treated at 25°C (Fig. 4a), a significant number of pits of approx. 1 µm in size can be noticed, which significantly increased the S_a up to 71.8 nm. With increasing temperature, a significant reduction in their formation was found, but on the surface much larger pits could be found (Fig. 4b). In further measurements, attention was paid to the progressive oxidation of the surface of austenite grains, characterized by an increasingly ragged surface of the samples (Fig. 4c–4f). The anodic polarization process, led to the removal of the grinding lines created after the mechanical polishing of the surface, but pitting was still present.

3.3. Selectivity of anodic polarization – chemical analysis of DES baths

The comparison of the chemical composition of the surface and the electrolyte, both "as-delivered" and after polarization, allows to determine whether the process was subject to selective oxidation of individual alloying elements, which is important for the polishing process itself and further surface properties, i.e., corrosion resistance. The main purpose of electrochemical polishing of steel alloys is to reduce roughness. In that process, alloying elements are etched from the surface, and a passive layer is formed. Table 2 presents the analysis of the content of selected elements in DES before and after the anodic polarization processes, performed on polarized samples at medium current densities, performed using the ICP-AES method.

From Table 2 it turns out that as the current density increases, the iron content in the solution increases. While the ratio of Fe : Cr in steel 304 is approx. 3.7 : 1, in the tested DES bath this value was almost twice as high, indicating a certain selectivity of the bath in the process of oxidation of elements on the sample surface. The same was with the ratio of Fe : Ni, which in selected steel is equal to about 7.5 : 1, and in the analyzed DES baths this ratio was much higher. On the other hand, the ratio of Cr : Ni in steel fluctuates around 2 : 1, which is a value similar to the value of the elements separated into the obtained solutions. The exception is the sample analyzed at 45°C, where relatively more nickel has passed into the solution. From Table 2 we can also conclude that the increase in temperature significantly increases the kinetics of the process. For instance, with the increase from 25°C to 75°C, the amount of iron and chromium that went into the solution

Table 3. XPS surface composition of the polarized sample (65°C, 15 mA cm^{-2}) and two samples, grinded and grinded + etched, as reference; samples analyzed in "as-received" form and after Ar^+ sputtering

Tabela 3. Skład powierzchni określony metodą XPS dla stali po polaryzacji (65°C, 15 mA cm^{-2}) i dwóch próbek referencyjnych, oszlifowanej oraz oszlifowanej i wytrawionej; próbki analizowano w postaci, w jakiej zostały dostarczone, i po trawieniu Ar^+

Surface treatment	Surface composition								
	Ni $2p_{3/2}$	Fe $2p_{3/2}$	Cr $2p_{3/2}$	O 1s	C 1s	Cr/Fe	Cr/Ni	Ni/Fe	O_{ox}/Me
Grinded	0.6	10.5	5.3	44.7	39.1	0.5	9.6	0.05	–
Grinded + Ar^+ sputtering	1.6	18.9	11.1	51.1	17.2	0.6	6.8	0.09	–
Grinded + chemical etching	0.3	6.3	4.7	46.1	42.7	0.8	15.7	0.05	1.9
Grinded + chemical etching + Ar^+ sputtering	0.9	15.6	9.9	53.5	20.0	0.6	10.7	0.06	–
Grinded + chemical etching + anodic polarization	0.7	5.7	5.6	39.6	48.4	1.0	7.9	0.12	1.4
Grinded + chemical etching + anodic polarization + Ar^+ sputtering	2.2	14.1	10.7	50.5	22.5	0.8	4.8	0.16	–

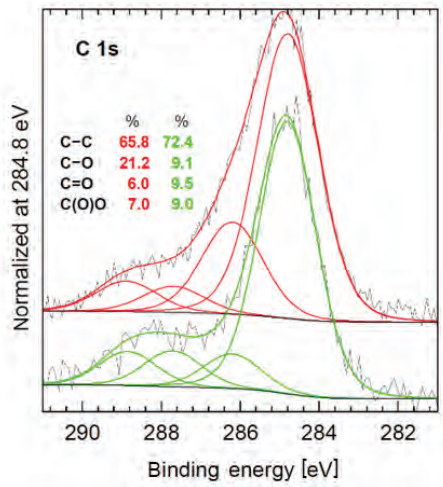

Fig. 5. C 1s spectra for grinded (red) and polarized (green) samples, analyzed in "as-received" state

Rys. 5. Widma C 1s dla próbki szlifowanej (czerwone) i próbki po polaryzacji (zielone), analizowanych w stanie, w którym zostały dostarczone

increased eight times, and nickel more than six times. The manganese content in the solutions after the electrochemical process was stable for all analyzed solutions. For the highest process temperature tested, compared to the starting solution, the manganese content increased almost twice. In the bath itself, the presence of copper could also be found, in amounts ranging from 0.12 ppm to 0.44 ppm, the content of which may counteract the effect of gas generation on the surface of the sample [22].

3.4. The effect of polarization in DES bath on surface chemistry – XPS analysis

For XPS analyses two reference samples were chosen: a grinded sample and a grinded and etched sample. This was necessary to analyze the change in surface composition as a result of the pre-treatment of the material. To determine the effect of the anodic polarization process on the surfaces, it was decided to focus on the sample polarized at 65°C and 15 mA cm^{-2}. Surface chemical composition of these samples is summarized in Table 3.

The surfaces of all samples were covered with a layer of natural oxides and adsorbed carbon compounds with a bond structure typical of metallic surfaces, namely C–C/C–H, C–O, C=O and CO_3/C(O)O (Fig. 5). The carbon contamination share on the surface of the grinded and etched samples was similar and amounted to approx. 40 at%. In the polarized sample, this share was higher (48%), which may have resulted from the contact of the steel surface with organic bath. The estimated thickness of the contamination carbon layer did not exceed 1 nm. It should be noted that the XPS technique is very surface sensitive, the sampling depth does not exceed the value of 3λ (inelastic mean free pathway for electrons, IMFP), and 66% of the analytical information comes from a layer only 1λ thick. In the case of the recorded photoelectron spectra of Ni 2p, Fe 2p, and Cr 2p in steel, the values of 1λ are 0.9 nm, 1.1 nm, 1.3 nm, respectively. The differences in the IMFP values explain the higher Cr : Fe ratios, especially Cr : Ni in the XPS analyzes (Table 3) compared to the nominal composition of the AISI 304 steel and they are the greater the thicker contamination layer is. Therefore, to better illustrate the differences in the structure of anodically polarized and chemically etched layers, Table 3 includes both the composition of the surface of the samples analyzed in "as-received" form and after sputtering with Ar^+ ion beam, as a result of which the carbon content decreased more than twice.

When analyzing the quantitative results, quite significant differences can be noticed between the samples. As could be expected, after selective chemical etching the Cr : Fe and Cr : Ni ratios increased by approx. 60%, with the Ni : Fe value unchanged. These dependencies are also preserved after Ar^+ sputtering. These results mean that chemical etching equally leaches both Fe and Ni from the alloy surface, enriching it with chromium. In the case of the surface of anodically polarized 304 steel in ChCl : OA a significant increase in the Cr : Fe ratio was also observed, from 0.5 to 1.0 (100%), but this time, the Ni : Fe ratio has also more than doubled. These values remained unchanged also after subsequent sputtering with Ar^+ beam. These results mean that the anodic polarization very selectively leaches only Fe from the steel surface.

The oxygen content in the passive layers of all samples was similar, ranging from 40–46 at%, and after partial removal of contamination carbon, this range narrowed to 50–53 at%. The absolute oxygen content, however, does not reflect the structure of covering the steel surface with a layer of native oxides, which has a direct impact on its anticorrosive properties. This is because a large part of the oxygen is related to adventitious/contamination carbon (Fig. 5). Taking into account the CO_x bonds, the degree of oxidation of the chemically etched AISI 304 steel surface turned out to be significantly higher than that of the polarized surface: the metal-bound oxygen ratio O_{MeOx} / Σ (Me_{ox} + Me) decreased from 1.9 to 1.4, respectively. The relatively lower amount of oxygen on the surface of the polarized steel was mainly due to the thinner layer of

Table 4. Spectral fitting for Cr species on the basis of Cr 2p percentage share spectra for grinded, etched, Ar^+ sputtered and polarized samples

Tabela 4. Dopasowanie widm Cr na podstawie składu procentowego widma Cr 2p dla próbek szlifowanych, trawionych chemicznie, polaryzowanych i trawionych Ar^+

Surface treatment	Spectra [%]				
	Cr(0)	Cr_2O_3	$Cr(OH)_3$	CrO_3	ΣCr_{oxides}
Grinded	20.9	26.4	69.0	4.6	79.1
Grinded + Ar^+ sputtering	23.2	31.4	63.7	5.0	76.8
Grinded + chemical etching	12.7	28.0	69.6	2.5	87.3
Grinded + chemical etching + Ar^+ sputtering	14.5	26.8	70.4	2.8	85.5
Grinded + chemical etching + anodic polarization	29.4	50.1	46.7	3.2	70.7
Grinded + chemical etching + anodic polarization + Ar^+ sputtering	29.8	56.5	41.0	2.5	70.2
Grinded + chemical etching + anodic polarization + Ar^+ sputtering + Ar^+ sputtering	32.9	53.3	43.2	3.5	67.1

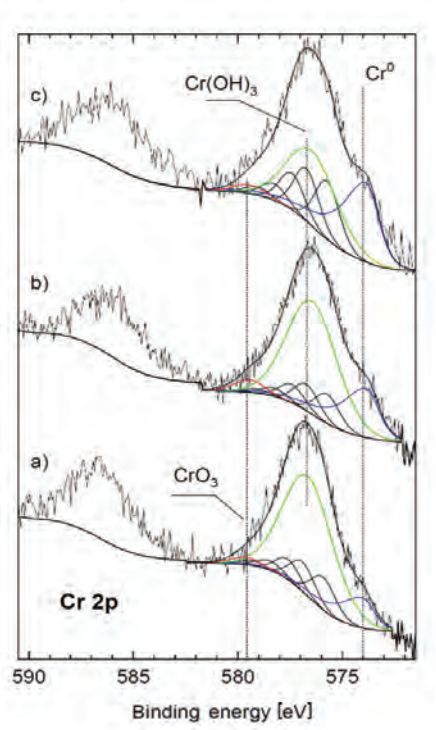

Fig. 6. Cr 2p spectra for samples analyzed in "as-received" form: a) grinded, b) chemically etched, c) polarized

Rys. 6. Widma Cr 2p dla próbek analizowanych w formie, w jakiej zostały dostarczone: a) szlifowanej, b) szlifowanej i trawionej chemicznie, c) po polaryzacji

native oxides and the resulting greater proportion of the metallic form in the substrate (Fig. 6, Table 4).

Figure 6 presents high-resolution Cr $2p_{3/2}$ spectra together with their deconvolution. During deconvolution of Cr 2p envelope, Cr(0), Cr(III) oxide, Cr(III) hydroxide and Cr(VI) components were assumed to exist and taken into account asymmetry in the metal peak. In the present work, the detailed procedure of Cr $2p_{3/2}$ spectra deconvolution described in the works of Biesinger et al. [23, 24].

When analyzing the results of the Cr $2p_{3/2}$ spectrum deconvolution, it is possible to notice not only a greater proportion of oxide species (thicker layer) on the chemically etched surface compared to the polarized surface, but also a different structure of chromium bonds. On the chemically etched surface, Cr(III) hydroxide is clearly dominant. Its share was estimated at approx. 70% of the total amount of oxidized chromium, while the content of Cr(III) hydroxide on the polarized surface was much lower and ranged from 41–47%. The share of Cr(III) oxide on both surfaces was 28% and 50%, respectively. For a better fit, the Cr(VI) component was also inserted (single peak at 579.5 eV – value averaged from literature data, FWHM ca. 1.7 eV). The share of Cr(VI) was estimated at approx. 3%. However, this estimate is not accurate due to low value and overlapping of Cr(VI) peak with multiplet splitting of the Cr(III) species.

The presence of metallic constituent, originating from the bulk of the coating, was used to estimate the passive layer thickness (d). The calculation was based on the Strohmeier equation (1) [25]:

$$d = \lambda_o \sin(\theta) \ln\left[\frac{N_{Cr}\lambda_{Cr}I_o}{N_o\lambda_o I_{Cr}} + 1\right], \quad (1)$$

where N is the number of atoms per unit volume, θ is the take-off angle of the electrons, λ is IMFP (inelastic mean free path) value for the electrons and I is the peak area. "Cr" and "o" indexes refer to metallic (bulk of the alloy) and oxidized (Cr_2O_3 oxide layer) components, respectively. In calculation, the presence of hydroxides ($Cr(OH)_3$) in the passive layer was also considered. Hence N_o and λ_o are the values of weighted arithmetic means [26, 27] of Cr_2O_3 and $Cr(OH)_3$ shares, resulting from the Cr $2p_{3/2}$ spectra deconvolution and I_o is the summary intensity of I_{oxide} and $I_{hydroxide}$. Finally, for grinded, grinded + chemically etched, and polarized samples, the thickness of the oxide layer was calculated to be: 3.8 nm, 4.5 nm, and 3.3 nm, respectively. Thus, the numerical values confirmed the earlier observations that out of the three tested surfaces, the oxide layer of the anodized sample was the thinnest. The applied model assumed a uniform mixture of oxides and hydroxides in the passive layer.

For the corrosion resistance measurements the same selection criteria for the samples were chosen as for the study of their surface composition using XPS. Therefore, two reference samples before the anodic polarization process were selected (grinded sample and mechanically grinded and etched sample) as well as a sample subjected to polarization process at 65°C and 15 mA cm^{-2}. Using the LPR method it was possible to estimate polarization resistance (R_p, Fig. 7). Analyzing the polarization resistance graph (Fig. 7a), we can observe that in the case of both reference samples, the way of their preparation has a rather insignificant effect on the change of R_p. The sample additionally chemically etched had a slightly higher corrosion resistance, which could be due to the etching of less noble elements from the surface of the sample, such as Fe. On the other hand, the sample subjected to the anodic polarization process was characterized by almost four times higher R_p value for the entire 24-hour corrosion resistance test. Thus, despite the deterior-

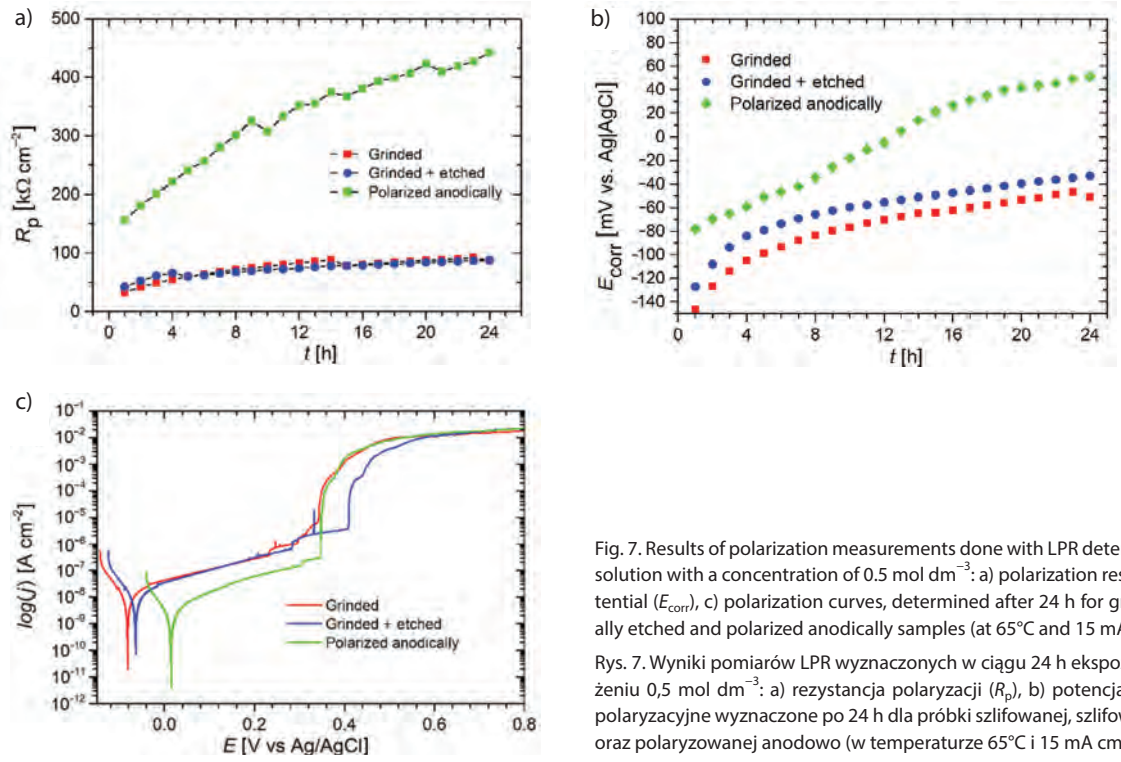

Fig. 7. Results of polarization measurements done with LPR determined during 24 h, in a NaCl solution with a concentration of 0.5 mol dm^{-3}: a) polarization resistance (R_p), b) corrosion potential (E_{corr}), c) polarization curves, determined after 24 h for grinded, grinded and chemically etched and polarized anodically samples (at 65°C and 15 mA cm^{-2})

Rys. 7. Wyniki pomiarów LPR wyznaczonych w ciągu 24 h ekspozycji w roztworze NaCl o stężeniu 0,5 mol dm^{-3}: a) rezystancja polaryzacji (R_p), b) potencjał korozyjny (E_{corr}), c) krzywe polaryzacyjne wyznaczone po 24 h dla próbki szlifowanej, szlifowanej i trawionej chemicznie oraz polaryzowanej anodowo (w temperaturze 65°C i 15 mA cm^{-2})

ation of the visual parameters of the steel surfaces of the samples, the anodic polarization process improved its corrosion parameters by creating a passive layer, demonstrated in XPS. By analyzing the corrosion potential, subjecting the samples to the anodic polarization process led to a shift of this potential in the positive direction (Fig. 7b). This value was ca. 51 mV for the polarized sample after 24 h, compared to the reference samples where the value was around –40 mV. The improved anticorrosion properties are related to the newly formed passive layer made of Cr and Ni compounds [28]. Higher corrosion resistance for the anodically polarized sample is ensured by the higher content of Cr^{3+} compounds (according to Table 4), whose leaching causes the corrosion processes to proceed [29]. On the polarization curves (Fig. 7c) it can be observed that each additional treatment of steel samples caused a shift of the transition potential towards the cathodic currents, while on each anodic branch a passive region was present. The width of this region varies, namely the polarized sample had the shortest passive region (~331 mV), and the grinded and chemically etched sample had the longest one (~471 mV).

From the EIS measurements (Fig. 8), it is possible to determine the rate of the processes taking place on the electrode and examine its surface. For the tested samples, three electrical equivalent circuits were proposed, two of which (model 1, for the "as-delivered" sample and for the anodically polarized sample) were the same (Fig. 8a). In the case of this model, the formation of an electrical double layer can be found. The resistor R_s is equal to the resistance of the liquid, and the elements R_1 and CPE correspond to the formation of an electrical double layer at the substrate-liquid interface. The elements R_2 and CPE1 are equal to the properties of the passive barrier layer, which has already been presented in the literature for 304 steel [30]. In the case of model 2 (for the sample after chemical etching), we can determine the poor anticorrosive properties and exposure of the substrate, which would be consistent with the preparation of the sample on which the oxide layer removal process by chemical etching was carried out. In the present arrangement, the resistor R_s is again responsible for the liquid resistance, and the elements R_1 and CPE layer represent the formation of an electrical double layer at the substrate-liquid interface. The present

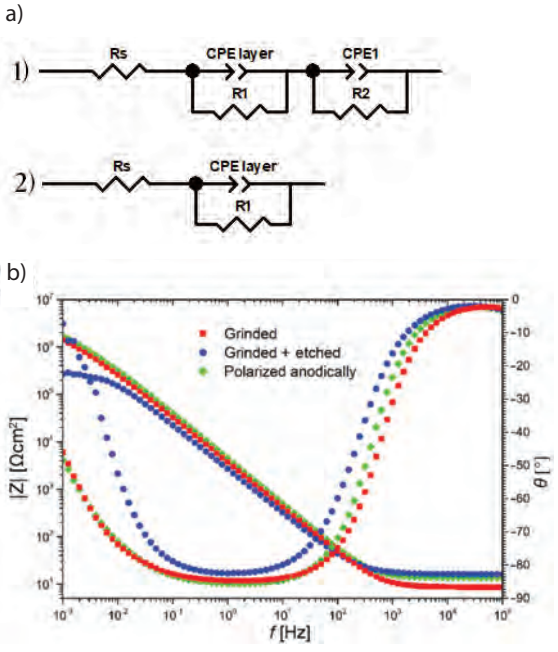

Fig. 8. EIS measurement results: a) equivalent electric circuits used to interpret the corrosion processes (1 – circuit used for samples grinded and polarized anodically at 65°C 15 mA cm^{-2}, 2 – circuit used for grinded and chemically etched sample), b) Bode spectra for the tested samples

Rys. 8. Wyniki pomiarów EIS: a) zastępcze obwody elektryczne służące do interpretacji procesów korozyjnych (1 – obwód stosowany w wypadku próbki szlifowanej i po polaryzacji anodowej w temperaturze 65°C, 15 mA cm^{-2}, 2 – obwód stosowany w wypadku próbki szlifowanej i trawionej chemicznie), b) widma Bodego dla badanych próbek

sample, according to the XPS analysis, consisted mainly of chromium(III) hydroxide which did not provide good barrier properties. The analysis of Bode spectra (Fig. 8b) confirms the present differences in the structure of passive layers formed on the surface of the samples, where the chemically etched sample has an order lower impedance than the other samples.

4. Conclusion

Deep eutectic solvent based on choline chloride and oxalic acid mixed in a 1 : 1 ratio was selected for the anodic polarization of the AISI 304 alloy steel. The process itself was carried out in the temperature range from 25°C to 75°C, with the current density ranging from 2.5 mA cm^{-2} to 45 mA cm^{-2}. It was found that:

- Along with the increase in the temperature and current density the number of pits on the surface of steel samples has increased, and thus their overall roughness increased. As researched, the roughness average (R_a) parameter of the samples could increase from 18 nm to even 339 nm.
- No improvement in visual parameters was observed, even when the roughness (R_a) was reduced to 12 nm (for sample polarized at 65°C and 2.5 mA cm^{-2}).
- AFM showed that the process carried out at lower temperatures (25°C and 35°C) led to the formation of evenly distributed shallow pits on the surface, and the increase in the temperature of the process to 45°C led to the formation of less numerous but larger pits. According to ICP-AES the DES proposed in this article acts very selectively on the iron etching of the samples, which led to the formation of numerous pits.
- XPS showed that the anodic polarization carried out in the tested DES bath increased the content of oxidized chromium on the surface of the samples, but with too high a degree of iron leaching. The applied model assumed a uniform mixture of oxides and hydroxides in the passive layer. However, in contrast to chemically etched steel surface, polarization in DES produces surface layer enriched with Cr_2O_3 with lower share of $Cr(OH)_3$. These qualitative differences reflected also in the thickness of passive layers: 4.5 nm for chemically etched steel, 3.8 nm for grinded steel and 3.3 nm for polarized steel.
- The produced passive layers, consisting of Cr^{3+} compounds, provided increased corrosion resistance, but overall visual parameters of the samples did not improved, which is one of the requirements of electrochemical polishing of alloyed steels.

Acknowledgements

The research was financed under the NCN MINIATURA II project entitled: "*Selektywne polerowanie elektrochemiczne stali stopowej typu 304 w przyjaznej środowisku mieszaninie eutektycznej chlorku choliny z kwasem szczawiowym lub cytrynowym*" – grant number 2018/02/X/ST5/01012 (contract number in Wrocław University of Science and Technology: 02NA/0006/18).

CRediT authorship contribution statement

Marek Marczewski: Investigation, Writing – original draft, Writing – review & editing.

Włodzimierz Tylus: Investigation, Writing – original draft, Writing – review & editing.

Juliusz Winiarski: Conceptualization, Funding acquisition, Resources, Writing – review & editing, Supervision.

BIBLIOGRAPHY

[1] J. J. Milledge. 2010. "The Cleanability of Stainless Steel Used as a Food Contact Surface: An Updated Short Review." *Food Science and Technology* 24(4): 27–28.

[2] A. K. Dewangan, A. D. Patel, A. G. Bhadania. 2015. "Stainless Steel for Dairy and Food Industry: A Review." *Journal of Material Science and Engineering* 4(5): 191. DOI: 10.4172/2169-0022.1000191.

[3] C. Jullien, T. Bénézech, B. Carpentier, V. Lebret, C. Faille. 2003. "Identification of Surface Characteristics Relevant to the Hygienic Status of Stainless Steel for the Food Industry." *Journal of Food Engineering* 56(1): 77–87. DOI: 10.1016/S0260-8774(02)00150-4.

[4] R. A. Covert, A. H. Tuthill. 2000. "Stainless Steels: An Introduction to Their Metallurgy and Corrosion Resistance." *Dairy, Food, and Environmental Sanitation* 20(7): 506–517.

[5] J. F. Frank, R. Chmielewski. 2001. "Influence of Surface Finish on the Cleanability of Stainless Steel." *Journal of Food Protection* 64(8): 1178–1182. DOI: 10.4315/0362-028X-64.8.1178.

[6] J. W. Arnold, G. W. Bailey. 2000. "Surface Finishes on Stainless Steel Reduce Bacterial Attachment and Early Biofilm Formation: Scanning Electron and Atomic Force Microscopy Study." *Poultry Science* 79(12): 1839–1845. DOI: 10.1093/ps/79.12.1839.

[7] S. Mohan, D. R. Kanagaraj, R. Sindhuja, S. Vijayalakshmi, N. G. Renganathan. 2001. "Electropolishing of Stainless Steel — a Review." *Transactions of the IMF* 79: 140–142. DOI: 10.1080/00202967.2001.11871382.

[8] G. Yang, B. Wang, K. Tawfiq, H. Wei, S. Zhou, G. Chen. 2017. "Electropolishing of Surfaces: Theory and Applications." *Surface Engineering* 33(2): 149–166. DOI: 10.1080/02670844.2016.1198452.

[9] W. Abdussalam-Mohammed, A. Qasem Ali, A. O. Errayes. 2020. "Green Chemistry: Principles, Applications, and Disadvantages." *Chemical Methodologies* 4(4): 408–423. DOI: 10.33945/SAMI/CHEMM.2020.4.4.

[10] E. L. Smith, A. P. Abbott, K. S. Ryder. 2014. "Deep Eutectic Solvents (DESs) and Their Applications." *Chemical Reviews* 114(21): 11060–11082. DOI: 10.1021/cr300162p.

[11] A. P. Abbott, G. Frisch, J. Hartley, W. O. Karim, K. S. Ryder. 2015. "Anodic Dissolution of Metals in Ionic Liquids." *Progress in Natural Science: Materials International* 25(6): 595–602. DOI: 10.1016/j.pnsc.2015.11.005.

[12] A. P. Abbott, K. S. Ryder, U. König. 2008. "Electrofinishing of Metals Using Eutectic Based Ionic Liquids." *Transactions of the IMF* 86(4): 196–204. DOI: 10.1179/174591908X327590.

[13] A. P. Abbott, G. Capper, K. J. McKenzie, A. Glidle, K. S. Ryder. 2006. "Electropolishing of Stainless Steels in a Choline Chloride Based Ionic Liquid: An Electrochemical Study with Surface Characterisation Using SEM and Atomic Force Microscopy." *Physical Chemistry Chemical Physics* 8(36): 4214–4221. DOI: 10.1039/B607763N.

[14] J. Winiarski, M. Marczewski, M. Urbaniak. 2021. "On the Anodic Polarization of 316 Steel in a Choline Chloride: Ethylene Glycol Deep Eutectic Solvent and Its Impact on the Surface Topography and Corrosion Resistance." *Ochrona przed Korozją* 64(1): 3–7. DOI: 10.15199/40.2021.1.1.

[15] M. Hayyan, M. A. Hashim, A. Hayyan, M. A. Al-Saadi, I. M. AlNashef, M. E. S. Mirghani, O. K. Saheed. 2013. "Are Deep Eutectic Solvents Benign or Toxic?" *Chemosphere* 90(7): 2193–2195. DOI: 10.1016/j.chemosphere.2012.11.004.

[16] J. Winiarski, M. Marczewski, W. Tylus. 2019. "Corrosion Resistance of 304 Stainless Steel after Anodic Polarization in Choline Chloride-Oxalic Acid Non-Aqueous Bath." *Ochrona przed Korozją* 62(3): 78–81. DOI: 10.15199/40.2019.3.3.

[17] A.-M. Popescu, V. Constantin, M. Olteanu, O. Demidenko, K. Yanushkevich. 2011. "Obtaining and Structural Characterization of the Electrodeposited Metallic Copper from Ionic Liquids." *Revista de Chimie* 62(6): 626–631.

[18] N. Dsouza, M. Appleton, A. Ballantyne, A. Cook, R. Harris, K. S. Ryder. 2014. "Removal of Casting Defects from CMSX-4® and CMSX-10® Alloys by Electropolishing in a Novel Electrolyte; Deep Eutectic Solvent." *MATEC Web of Conferences* 14: 13007. DOI: 10.1051/matecconf/20141413007.

[19] ISO 4301-304-00-I.

[20] A.-M. Popescu, C. Donath, V. Constantin. 2014. "Density, Viscosity, and Electrical Conductivity of Three Choline Chloride Based Ionic liquids." *Bulgarian Chemical Communications* 46(3): 452–457.

[21] E. Łyczkowska-Widłak, P. Lochyński, G. Nawrat. 2020. "Electrochemical Polishing of Austenitic Stainless Steels." *Materials* 13(11): 2557. DOI: 10.3390/ma1311255.

[22] D. J. Arrowsmith, A. W. Clifford. 1980. "The Influence of Copper on the Electropolishing of Stainless Steel." *Transactions of the IMF* 58(1): 63–66. DOI: 10.1080/00202967.1980.11870527.
[23] M. C. Biesinger, B. P. Payne, A. P. Grosvenor, L. W. M. Lau, A. R. Gerson, R. S. C. Smart. 2011. "Resolving Surface Chemical States in XPS Analysis of First Row Transition Metals, Oxides, and Hydroxides: Cr, Mn, Fe, Co, and Ni." *Applied Surface Science* 257(7): 2717–2730. DOI: 10.1016/j.apsusc.2010.10.051.
[24] http://www.xpsfitting.com/search/label/Chromium (access: 28.05.2021).
[25] B. R. Strohmeier. 1990. "An ESCA Method for Determining the Oxide Thickness on Aluminum Alloys." *Surface and Interface Analysis* 15: 51–56. DOI: 10.1002/sia.740150109.
[26] M. C. Biesinger, B. P. Payne, L. W. M. Lau, A. Gerson, R. S. C. Smart. 2009. "X-ray Photoelectron Spectroscopic Chemical State Quantification of Mixed Nickel Metal, Oxide, and Hydroxide Systems." *Surface and Interface Analysis* 41(4): 324–332. DOI: 10.1002/sia.3026.
[27] A. Laszczyńska, W. Tylus, J. Winiarski, I. Szczygieł. 2017. "Evolution of Corrosion Resistance and Passive Film Properties of Ni-Mo Alloy Coatings during Exposure to 0.5 M NaCl Solution." *Surface and Coatings Technology* 317: 26–37. DOI: 10.1016/j.surfcoat.2017.03.043.
[28] V. Zatkalíková, L. Markovičová. 2019. "Corrosion Resistance of Electropolished AISI 304 Stainless Steel in Dependence of Temperature." *IOP Conference Series: Materials Science and Engineering* 465(1): 012011. DOI: 10.1088/1757-899X/465/1/012011.
[29] S. Gao, C. Dong, H. Luo, K. Xiao, X. Li. 2014. "Electrochemical Behavior and Nonlinear Mott-Schottky Characterization of a Stainless Steel Passive Film." *Analytical Letters* 47(7): 1162–1181. DOI: 10.1080/00032719.2013.865201.
[30] F. Mohammadi, T. Nickchi, M. M. Attar, A. Alfantazi. 2011. "EIS Study of Potentiostatically Formed Passive Film on 304 Stainless Steel." *Electrochimica Acta* 56(24): 8727–8733. DOI: 10.1016/j.electacta.2011.07.072.